International Journal of Hydrogen Energy 110 (2024) 677–686

Contents lists available at ScienceDirect

International Journal of Hydrogen Energy

journal homepage: www.elsevier.com/locate/he

Effect of sorghum biomass on hydrothermal co–gasification of PET/HDPE/PP/PVC for hydrogen production

Şefika Türker Üzden *, Ender Fakı, Açelya Seçer, Arif Hasanoğlu *

Çukurova University, Faculty of Arts and Sciences, Chemistry Department, Turkey

ARTICLE INFO

Handling Editor: Dr Mehran Rezaei

Keywords:
PET
PP
HDPE
PVC
Sorghum
Hydrothermal gasification
Hydrogen

ABSTRACT

This study investigated the effects of sorghum biomass (SB) on the hydrothermal co–gasification (HcG) of polyethylene terephthalate (PET), high–density polyethylene (HDPE), polypropylene (PP), and polyvinyl chloride (PVC). The gasification trials of both individual plastics and SB as well as P/SB combinations were conducted. The effects of adding SB to plastic HcG on total gas volume, mole fraction distribution, hydrogen efficiency, gasified carbon conversion and liquid analysis were examined. The total gas volume obtained from hydrothermal gasification (HG) of individual plastics ranked as PP > PET > HDPE > PVC. In contrast, during HcG, the order changes to PVC/SB > PP/SB > PP/SB > HDPE/SB > PET/SB. The hydrogen efficiency ranking for individual plastics is PP > HDPE > PVC > PET. The hydrogen efficiency of PP is 14.5 (±0.3) mol H_2/kg feed. The order of hydrogen efficiency for co–gasification is PVC/SB > HDPE/SB > PP/SB > PET/SB. 16.9 (±0.2) mol H_2/kg feed was obtained from co–gasification of PVC/SB, and 20.3 (±0.3) mol H_2/kg feed was obtained with the catalyst. The greatest H_2 efficiency increase of 6.0 mol H_2/kg feed was observed when catalytic conditions replaced HcG of PET/SB. According to GC–MS analysis, aromatics and furfural derivative structures have created shift effects towards phenolic compounds by reducing the product variety in liquid analysis. The study was investigated to determine the effective combination of different types of plastics with biomass for hydrogen rich gas production via HcG. It is envisaged that the use of KCl, one of the most abundant salts in seawater, as a catalyst and the use of plastic wastes as input without any drying and washing process before gasification may have a cost–cutting effect on expensive hydrogen technologies.

1. Introduction

Plastics have become integral to modern life, owing to their versatility, durability, and cost–effectiveness. Since the mid–20th century, they have been widely utilized across various industries, including packaging, construction, automotive, electronics, food, and healthcare sectors [1,2]. PVC, PET, PP and HDPE are some of the most widely produced and used plastics that serve a wide range of applications. For instance, PVC is recognized for its cost–effectiveness and exceptional durability. The versatility of processing techniques has made it one of the most widely used thermoplastic polymers worldwide, with applications ranging from window frames, doors, and wall panels to pipes, cable insulation, furniture, and medical devices [3,4]. Similarly, PET is predominantly used in beverage bottles and food packaging, because of its excellent clarity, strength, and flexibility [5,6]. HDPE is one of the largest–volume commodity chemicals among plastics. Molding is widely used in the production of bottles, household items, toys, supermarket bags, and automotive parts. PP, having a similar structure, is a versatile polymer that is preferred for the production of films and fibers [7]. The groups with the largest share in non–fibre plastic production are PE 36%, PP 21%, PVC 12% and PET <10% [8].

Global plastic production, which was approximately 2 million tonnes in 1950, surged to over 450 million tonnes by 2019 [9] and if this upward trend continues, it is projected to exceed 1000 million tonnes by 2050 [10]. The increasing use of plastics during the COVID–19 pandemic, particularly for masks, gloves, and other disposable personal protective equipment, underscores their undeniable contribution to healthcare due to their durability and adaptability. Despite these benefits, concerns about plastic waste and regulation continue globally [11]. The persistence of plastics, which can take 100 to 1000 years to decompose, exacerbates the problem as most of the plastics ever produced are likely to still be in the environment today [12]. The severe environmental impacts of plastic pollution have prompted urgent calls for alternative waste management strategies that minimize harm while recovering the value of plastic waste. The various advanced

* Corresponding authors. Çukurova University, Faculty of Arts and Sciences, 01130, Adana, Turkey.
E-mail addresses: sefikaturker2@gmail.com (Ş. Türker Üzden), ahesenov@cu.edu.tr (A. Hasanoğlu).

https://doi.org/10.1016/j.ijhydene.2025.02.179
Received 11 December 2024; Received in revised form 2 February 2025; Accepted 10 February 2025
Available online 21 February 2025
0360-3199/© 2025 Hydrogen Energy Publications LLC. Published by Elsevier Ltd. All rights are reserved, including those for text and data mining, AI training, and similar technologies.

List of abbreviations:

daf	dry, ash–free
DTG	Derivative Thermogravimetry
HDPE	High–Density Polyethylene
HG	Hydrothermal Gasification
HcG	Hydrothermal Co–gasification
LHV	Lower Heating Value
PET	Polyethylene Terephthalate
PP	Polypropylene
PVC	Polyvinyl Chloride
P/SB	Plastics and Sorghum
SB	Sorghum Biomass
TGA	Thermogravimetric Analysis
wt	weight

optimization and modeling techniques, such as the orthogonal array of Taguchi approach, response surface methodology (RSM), and multi–criteria decision–making (MCDM) analysis, have demonstrated significant potential in enhancing the understanding and efficiency of plastic waste gasification processes under diverse conditions [13–16]. One of the promising approaches is hydrothermal gasification (HG), a process capable of converting plastics and biomass into hydrogen–rich gases [17,18], addressing both plastic waste disposal and sustainable energy production. HG uses the unique physicochemical properties of subcritical or supercritical water. The fact that water acts as a solvent, catalyst and reagent distinguishes this process from other methods. In terms of mechanism, different chemical pathways such as ionic and radical reactions are prominent in HG [19–25]. This technology produces hydrogen as a valuable by–product with the potential to degrade various plastics and biomass materials [17,18,26,27]. Hydrogen stands out as a promising clean energy source due to its exceptional energy to weight ratio, high calorific value of 120–142 MJ/kg, and ability to generate energy without emitting carbon during combustion [28]. However, it is expensive due to its high production costs, difficulties in storage and transportation, extensive infrastructure requirements, and limited scale of use. Today, the cost of renewable hydrogen production is 1.5–6 times higher than hydrogen production from fossil fuels [29]. Often touted as the fuel of the future, hydrogen is an attractive option for clean energy production as it produces no carbon emissions during combustion. Therefore, integrating hydrogen production with plastic waste management offers a promising solution to two important global challenge [30]. Recent research has shown that co–gasification, which involves mixing plastics with biomass, can increase hydrogen production due to synergistic effects among the materials [31–33]. Thus, it offers a valuable strategy that also addresses environmental sustainability goals, yet it presents several challenges that must be addressed to optimize the process. A significant challenge lies in the diversity of plastic types, each with distinct thermal properties and chemical compositions, complicating their processing and integration into a unified gasification system. Additionally, understanding the potential synergistic effects when combining different plastics with biomass is crucial for enhancing process efficiency. The optimization of process parameters, particularly through the use of catalysts, is essential to improve gasification outcomes such as hydrogen production and carbon conversion. Furthermore, it is important to investigate how various plastic types and their combinations behave under specific gasification conditions to develop effective strategies for mixed waste streams.

In this study, the effects of KCl catalyst were investigated on the HcG of PET, PP, HDPE and PVC, which are widely used and contribute significantly to terrestrial plastic wastes, with sorghum biomass (SB). Every year, 1.15 to 2.41 million tons of plastic waste enters the ocean from rivers [34]. Approximately 80 % of plastic waste are transported from land to the ocean [35]. PET, HDPE, PP and PVC are among the most widely used and discarded plastics globally and represent a significant proportion of plastic waste [36,37]. PET is classified as a polycondensation polymer, whereas HDPE, PP, and PVC are categorized as polyolefin polymers. Their selection was chosen to ensure the relevance of the study in terms of addressing real–world waste management challenges. The partial molar volume of KCl is known to be 29.39 cm^3/mol under typical seawater conditions (SA = 35.165 g/kg) at 25 °C [38,39]. The direct inclusion of plastic wastes into the HG process by collecting them from the ocean and using them without prior drying or desalination is critical in terms of both energy efficiency and cost–effectiveness. Therefore, KCl was selected as the catalyst, and HG was used as the gasification method. SB is highly diverse, comprising a total of 48 different taxa, including 31 cultivated species and 17 related wild species [40]. SB, an energy product known for its durability in arid lands, renewable nature, and high lignocellulosic content, was selected as a biomass source due to its possible synergistic effects with plastics during gasification. Thus, when the production of hydrogen–rich gas is targeted using plastic waste as input, it becomes an alternative solution to the waste problem, while SB becomes a unique companion due to both its synergistic effects and its sustainable and renewable features. The P/SB utilises the strengths of the two feedstocks to ensure the efficiency and sustainability of the process. That is, in hydrothermal co–gasification, P/SB combinations were selected to study the synergistic effects between them and maximize hydrogen production. The previous studies have not investigated the effects of four common plastic types, either separately or together with biomass, on hydrogen efficiency, total gas volume, carbon conversion, and liquid product analysis under HG conditions at varying temperatures (400, 450, and 500 °C) using KCl catalyst. Furthermore, the efficiency of alkali catalysts such as KCl varies depending on the specific combination of plastic and biomass used and operational operating conditions such as temperature and pressure. Understanding these variables is essential to maximize and optimize the benefits of catalytic gasification.

2. Materials and methods

2.1. Materials

SB (referred to as Green Go) grown at Cukurova University Agricultural Research Areas in Adana was used as a biomass source. The harvested SB was ground into small pieces (≤140 mesh) for use in the experiments. The virgin PET, PP, HDPE, and PVC were used as plastic materials. KCl was obtained from Sigma Aldrich and used as a catalyst, while distilled water served as the solvent and reagent in the processes. The elemental analyses of the plastics and SB were determined by a Thermo Scientific Flash 2000 instrument. Detailed analytical information on the results of the proximate and final analyses for plastics and SB can be found in Table 1. The findings in Table 1 were close to or consistent with the literature [41].

Table 1
Detailed analytical information on the results of the proximate and final analyses for plastics and SB.

	SB	PET	PP	HDPE	PVC
C (wt %, dry)	39.8	62.9	88.1	87.3	32.7
N (wt %, dry)	0.8	0.0	0.0	0.0	0.0
H (wt %, dry)	5.2	4.2	11.9	12.7	3.9
Cl (wt %, dry)	nd	0.0	0.0	0.0	63.4
O[a] (wt %, dry)	45.8	32.9	nd	nd	nd
Moisture (wt %)	8.1	nd	nd	nd	0.2
Ash (wt %, dry)	8.4	nd	nd	nd	nd
Volatile matter (wt %, dry)	81.4	89.9	99.4	100.0	83.9
Fixed carbon (wt %, dry)	18.9	11.4[b]	0.05 [b]	0.05 [b]	7.7 [b]
High heating value (MJ/kg, dry)	18.3	22.9 [b]	47.3[b]	48.0[b]	17.8[b]
Lower heating value (MJ/kg, dry)	17.3	22.0[b]	44.1[b]	40.0[b]	16.8[b]

nd: not determined; [a] calculated from difference; [b] data from [42].

2.2. Method

Gasification experiments were carried out in a stainless–steel batch–type reactor (Parr Model 4575 H P/TP, manufactured by Parr Instrument Co., Moline, IL) with a total volume capacity of 100 mL. The operating conditions were selected based on previous studies and preliminary experiments conducted for this study [27]. In the previous study, 25 mL of water and 3% (w/w) catalyst were found to be suitable for the highest hydrogen yield and the same parameters were used in this experimental process [27]. The preliminary experiments were conducted with different feed ratios (1:1; 1:2; 1:3) and 1:1 ratio was selected. The reactor was purged with 440 psi N_2 to remove the air inside of the reactor before starting the experiment. There was no positive pressure from the N_2, so there was no effect on the total gas volume. To study the effect of temperature on gasification, the reactor pressure was determined between 400 and 500 °C to maintain operational applicability without compromising the operating conditions. The heating process was initiated at room temperature and the system was heated to the target temperature of 500 °C at a rate of 10 °C per minute with continuous stirring at 1000 rpm. The duration of the HG experiments was 30 min after reaching the target temperature. Once the reaction time was over, the reactor was immersed in a container filled with water and rapidly cooled to room temperature. Each experiment was performed in triplicate, and the standard deviations and mean values were calculated from the results. The gaseous products generated during the gasification experiments were collected in a water–filled glass burette. The collected gaseous mixture was analysed by Gas Chromatography (GC). A dual–channel Varian 450 series GC instrument equipped with a dual TCD detector and a Supelco Carboxen 1010 PLOT FUSED SILICA capillary column (30 m length, 0.32 mm inner diameter) was used to qualitatively and quantitatively analyse the components. Comprehensive details on the analysis of the gas products can be found in previous studies [27]. The liquid products were extracted with dichloromethane to determine the organic components using a Thermo TR–5MS capillary column (60 m length, 0.25 mm internal diameter, 0.25 μm film thickness) connected to a Thermo Finnigan Gas Chromatography–Mass Spectrometry (GC–MS) instrument [43]. For moisture (wt%) and ash (wt %), dry) analysis, ASTM D 7582–15; for fixed carbon (wt%), dry) analysis, ASTM D 3172–13 method was used. Thermogravimetric analysis (TGA) of virgin plastics and SB were performed using a Mettler Toledo TGA–DSC 3+ Model (Serial No: B733518366) instrument with a N_2 flow rate of 40 mL/min from 25 °C to 1000 °C in 15 °C/min increments (see Fig. 1).

3. Results and discussion

3.1. Impact of feedstock variability on hydrothermal gasification performance

3.1.1. Effect of SB on the HcG of plastics

In this part of the study, HG experiments were initially conducted separately for PET, PP, HDPE, PVC and SB. The aim of this approach is to provide a basis for analytical comparison of total gas volume, product distributions and liquid analysis by plastic type in the HcG of SB. Fig. 2 shows the total gas volumes and product distributions resulting from the separate and co–gasification of both plastics and SB.

During HG, water at high temperature and pressure can facilitate hydrolysis, in addition to its increased density for competing reactions and because it moves towards a lower viscosity similar to a gas [44]. Considering that the gasification performances of different materials are unique, the distributions of H_2, CO, CH_4, CO_2 and C_2H_6 in the gas mixtures produced in all experiments are different. The total gasification volume of SB was 438 (±26) mL and contained 51.4 % (±0.3) H_2. Comparing the gasification results of plastics, PVC had the highest mole fraction of hydrogen 71.8 % (±1.7). Polyenes, formed as intermediates during the hydrothermal gasification of PVC, had been reported to degrade in SCW, undergoing hydrogen abstraction, cyclization, aromatization, and hydration reactions, ultimately leading to the formation of various hydrocarbons in the oil phase. Consequently, in addition to an increased oil phase, the enhancement of gasification and decarboxylation reactions has been linked to a higher gas yield [45]. According to TGA, since PVC starts to decompose lower temperatures than other plastics, the gas yield may have increased due to the fact that the formed structures are exposed to relatively more interaction in HG and HcG. The total gas volume of PVC was 364 (±11) mL. However, since the total gas volume of PP with 65.6 (±0.8) percent H_2 efficiency was 541 (±24) mL,

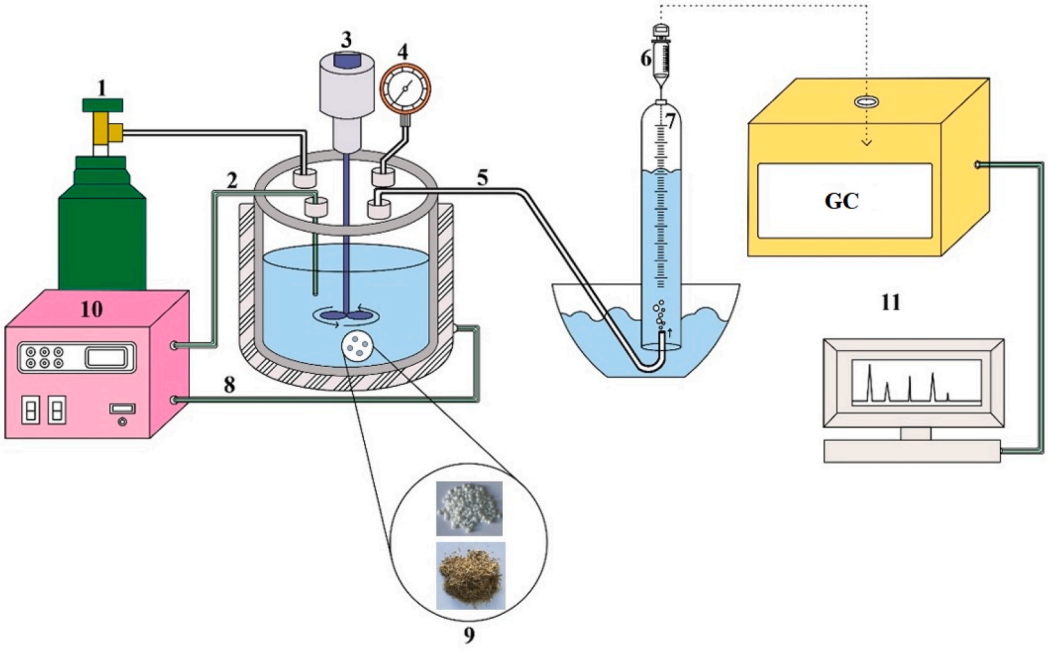


Fig. 1. Scheme of the co–gasification process (1) purge gas, (2) thermocouple, (3) stirring system, (4) pressure gauge, (5) gas compressor line, (6) injector, (7) gas collector, (8) batch reactor and furnace, (9) plastic/SB mixtures, (10) control unit, (11) Gas Chromatography.

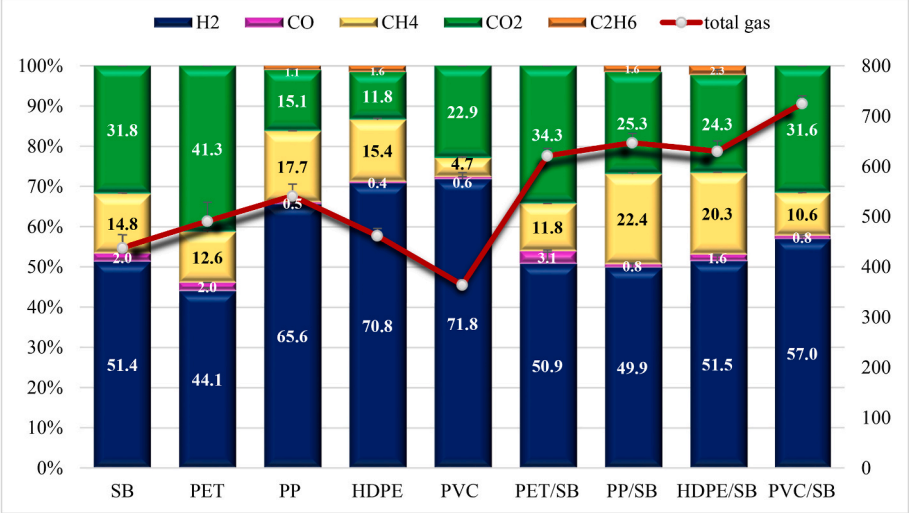


Fig. 2. The comparison of total gas volumes and product distributions of separate and co–gasification of PET, PP, HDPE, PVC and SB.

the highest H_2 efficiency by volume belonged to PP with 355 (±9) mL. HDPE ranks second with a hydrogen volume of 327 (±10) mL and the H_2 mole fraction is 70.8 % (±0.9). The chemical structures of PET and HDPE are very different from each other. When the results of 'proximate and final analyses' are examined, there are serious differences in terms of the percentages of C, H and O they contain. While the C, H and O contents of PET are 62.9%, 4.2% and 32.9% respectively, the carbon percentage of HDPE is 87.3% and hydrogen percentage is 12.7%. The reason for more hydrogen formation in the experiment using HDPE is related to the fact that the percentage of hydrogen in the HDPE structure is three times higher than the hydrogen in PET. HDPE and PP are hydrocarbon polymers with no oxygen in its structure, facilitating hydrogen–rich gas production during thermal breakdown. PET, on the other hand, contains oxygen in its ester groups, leading to competing reactions that produce CO_x gas products. It had been reported that PET, despite having readily cleavable oxygen bonds in its main chain, predominantly reverts to its original monomers due to the stability of its benzene rings [46]. Also, according to the TGA result, almost all components of PP and HDPE were thermally decomposed at about 500 °C. This may indicate that the structures decomposed by subjecting these plastics to HG at 500 °C contribute significantly to the gasification efficiency. The total gas volume obtained from the HG of PET is 491 (±38) mL. Under the conditions of this study, PET exhibited the lowest mole percentage of H_2 at 44.1 (±0.7). Considering the TGA of PET, the degradation starts at about 400 °C and decomposes in a wide range up to 640 °C. In addition, benzene and biphenyl formed by decarboxylation in the gasification reactions of PET are tar products sensitive to high temperatures [47]. This may have caused the H_2 efficiency from PET HG to be lower compared to other plastics. While PET HG produced 41.3% (±1.1) CO_2, SB HG produced 31.8% (±0.4) CO_2. The CO yield remained below 2 %. When CH_4 distributions were compared, PP gave the highest concentration with 17.7 (±0.1) %, while PVC had the lowest concentration with 4.7 (±0.3) %.

The gas with the highest mole fraction in separate and co–gasification was H_2. PVC/SB was the leader among HcG combinations with 57.0% (±0.5). When PVC and PVC/SB were compared, although H_2 efficiency decreased by 14.8 % in HcG according to mole fraction distribution, since the total gas volume increased to 725 (±15) mL, the H_2 amount by volume reached the highest distribution with 413 (±9) mL. Biomass is considered to enhance the dechlorination of PVC plastics, as its hydroxyl groups can substitute chlorine atoms, while also inhibiting PVC particle aggregation [48]. Moreover, the acidic environment generated during the hydrothermal dechlorination of PVC may further facilitate biomass hydrolysis [21]. It was observed that the hydrogen mole fractions formed in SB with PET and HDPE mixtures were approximately 51–52%. PET/SB and PVC/SB mixtures showed the highest CO_2 mole fractions with 34.3 % (±2.7) and 31.6 % (±0.7). While the previous study presented gasification data for PET, SB and PET/SB [27], in this study data was added to compare the effect of SB on 4 different plastics in HcG. In the gasification of plastics separately, PP had the highest total gas volume and hydrogen content. However, the H_2 % value of the PP/SB mixture decreased to 49.9 % (±1.1). Despite an increase of 106 (±7) mL in total gas volume, there was a decrease of 31 (±3) mL in hydrogen efficiency. The significant gas composition profiles with the highest CH_4 production belonged to PP/SB (22.4 ± 0.4%) and HDPE/SB (20.3 ± 0.2%). Alkali salts present in biomass may have catalyzed the recombination of CH_4 and C_2H_6, originating from the depolymerization of HDPE and PP [49]. The increased CH_4% observed in HDPE/SB and PP/SB mixtures supports this assumption.

These plastics typically have higher carbon and hydrogen content compared to SB. With the addition of SB to plastic gasification, the oxygen content in the structure can increase the formation of oxygenated components such as CO_2, CO. The CO% amount for each P/SB mixture was found to be in the range of 3–1%. Among the tested combinations, the non–catalytic PVC/SB mixture stood out as a particularly advantageous option in terms of hydrogen efficiency. According to TGA, the decomposition onset temperatures of all plastics were higher than that of SB. For biomass, volatile matter loss started at lower temperatures (150–200 °C), where hemicelluloses (150–350 °C), cellulose (275–350 °C) and lignin (250–500 °C) degraded respectively [50]. The experiments were heated starting from room temperature up to the target temperature. It is thought that the radical intermediates formed during the decomposition of biomass accelerate the gasification process for plastics. Hydroxyl and carbonyl functional groups in cellulose and hemicellulose structures are thought to contribute to more efficient gasification reactions by increasing the degradation of plastic molecules in the gasification medium. This can be attributed to the fact that inorganic components naturally present in biomass, especially alkali and alkaline earth metals, can act as catalysts that reduce the activation energy required for decomposition reactions and increase the gasification rate [51,52]. Plastics can provide abundant H· radicals to favour hydrogen formation in the gasification process with biomass. The H· radicals formed can interact with species produced by the breakdown of biomass and accelerate the decomposition of complex hydrocarbons such as aromatic compounds [53]. Overall, co–gasification under these conditions provided a mutually positive contribution in terms of total volume compared to separate gasification of SB and plastics.

The composition of liquid products resulting from the gasification

experiments of separate SB and plastic species was analysed by GC–MS. The liquid products were categorized according to their chemical structure and functional groups, the data provided in Table 2.

The liquid product obtained from HG of SB contained predominantly phenolic derivatives (phenol, p–cresol, and m–ethylphenol). In addition, furfural, a furanoid compound that is commonly formed as a result of the thermal degradation of hemicellulose, at a rate of acetophenone, is a compound mainly obtained from the thermal degradation of lignin and its derivatives, constituted of the liquid part in relative terms [54,55]. Generally, olefins undergo additional reactions to generate cyclic and aromatic compounds, facilitated by cyclization via double bonds and subsequent dehydrogenation, as these structures exhibit greater stability [46]. Aromatic compounds such as toluene and phenol (phenol, p–cresol) obtained from gasification of HDPE are characteristic products of thermal decomposition of HDPE. Toluene, xylene isomers and other aromatic hydrocarbons and long–chain alkanes were found from gasification of PP. While aliphatic ketones such as 2–methyl–2–pentanone were prominent in the products obtained from gasification of PVC, various aromatic hydrocarbons (ethyl benzene, m–xylene and naphthalene), furfural and phenol were detected in significant amounts. (R)–benzyl–α–chloride, which is thought to be formed by the presence of chlorine in the structure of PVC, was detected. In the liquid products of HG of PET, mainly o–cresol and ketone groups were identified. The results show the diversity of products formed during gasification of plastics and SB. The GC–MS results of P/SB without catalyst were discussed in the following section for comparison with the P/SB experiments conducted with KCl.

3.1.2. Effect of KCl on the HG and HcG of P/SB

In this part of the study, both individual HG and HcG of PET, PP, HDPE and PVC with SB were carried out in the presence of KCl catalyst. In the presence of catalyst, SB, total gas volume increased but no major changes occurred in the percentage distribution of gases. H_2 (52.2 ± 0.6%) gas volume increased by 44 ± 6 mL and CO_2 (33.2 ± 0.7%) gas volume increased by 32 ± 7 mL. While there was no significant change in CO and volume, CH_4 decreased to 12.2% (±0.3). According to these results, the catalyst may have favoured the vapour gasification reaction for SB. When comparing the % H_2 between plastics, there was a small increase in PET (44.9 ± 0.8%). There was a decrease in PVC (67.9 ± 0.8%), PP (62.9 ± 0.4%) and HDPE (68.1 ± 1.0%). H_2 gas volumes increased in all plastic types, although the % values decreased in each plastic due to the increase in total gas volume ranging between 97 and 47 mL. CO_2 increased in PVC (23.5 ± 0.6) and PET (42.6 ± 0.9) and decreased in HDPE (9.7 ± 0.4) and PP (13.0 ± 0.3). CO amounts varied between approximately 3–1%. The literature indicated a low CO gas fraction in the presence of KCl [23]. The amount of CH_4 decreased in PET (9.6 ± 0.4) and increased in other plastic types used. As a result of HDPE (4.0 ± 0.2) and PP (3.3 ± 0.1) HG, $\%C_2H_6$ values were determined in gas mixtures and increased compared to the results without catalyst. The effect of SB in the presence of KCl on the co–gasification performance of the plastics was assessed in terms of total gas yield, gas composition distribution, and liquid analysis. Fig. 3 is given together to compare the total gas volumes and mole fraction percentages of HcG of P/SB without catalyst and with KCl.

The highest total gas volume of the trials of the P/SB mixture containing KCl catalyst belonged to PVC/SB (858 ± 17 mL). There was no significant change in the H_2 percentage of PVC/SB. However, the H_2 volume increased by 84 (±7) mL due to the 133 (±14) mL increase in the total gas volume. CH_4 amount increased by 3.5 %, CO_2 amount decreased by 4.9 % and no significant change was observed in CO % ratio. Rising temperatures favour methanisation and cracking reactions [56,57]. Considering the decreasing % CO_2 amount, it is thought that CO_2 supports methanation reaction [$CO_2 + 4H_2 \leftrightarrow CH_4 + 2H_2O$] and causes an increase in CH_4 amount [58]. Total gas volume increased by 52 (±9) mL in PP/SB mixture and 41 (±6) mL of this increase was in H_2 direction. However, there was no significant change in the distribution percentages of other gas fractions. Total gas volume rose by 97 (±10) mL in HDPE/SB combination. This increase was mainly in H_2 and CO_2 directions. CH_4 % amount decreased by 1.9 %. The % CH_4 amount decreased in PET/SB and HDPE/SB mixture. This situation was thought to be due to the triggering of KCl steam reforming reaction [$CH_4 + H_2O \leftrightarrow CO_2 + 3H_2$]. In the PET/SB combination, the total gas volume increased by 151 (±11) mL and reached 772 (±29) mL. The H_2 % ratio of PET/SB exhibited the largest rate of increase (rising by 9.0 %) to reach 59.9 (±0.4) %. The decrease of 2–3% was observed in the CO % and CH_4 % fractions and the CO_2 volume increased by 27 (±3) mL. This difference can be explained by the potential reactions that occur during the HcG process. In all combinations where KCl was added, there was an increase in the total gas volume with increases ranging from 52 to 133 mL. The maximum pressure observed during gasification was 3600 psi. It has been reported that K^+ ion facilitates the Boudouard reaction ($C + CO_2 \leftrightarrow 2CO$) and reduces tar formation [51]. The elevated CO amount may have enhanced H_2 production by supporting the water–gas shift reaction ($CO + H_2O \leftrightarrow H_2 + CO_2$) [59,60]. It was observed that this effect was the highest in terms of H_2 in the PET/SB mixture. It can be stated that in the presence of KCl catalyst, PVC/SB and PET/SB mixtures provide advantages in terms of H_2 production. HG experiments with KCl were also carried out for single SB, PET, PP, HDPE and PVC. When individual HcG experiments with and without catalysts were compared, the highest increase in total gas volume and H_2 yield was observed for PVC and SB (97 (±8) and 77 (±5) respectively) However, this increase was not as large as in the P/SB HcG experiments, which was attributed to the synergistic effects of the presence of biomass in the P/SB HcG experiments increasing the KCl efficiency. KCl may have interacted with naturally occurring minerals in the biomass to form more effective catalytic sites [61]. The % CH_4 amount decreased in PET/SB and HDPE/SB mixture. This situation is thought to be due to the triggering of KCl steam reforming reaction [$CH_4 + H_2O \leftrightarrow CO_2 + 3H_2$]. There was no significant change in PP/SB. However, due to the catalytic effect of KCl on PVC/SB, CH_4 efficiency increased. Chlorine atoms in the PVC structure may have interacted with KCl and affected radical reactions and hydrogen transfer mechanisms. Thus, it may have facilitated the stabilization of intermediate products and hydrogen bonding reactions. The methanation reaction in SCW, considering the decreasing % CO_2

Table 2
Classification and distribution of liquid products generated by gasification of individual plastics and SB.

Compound	Aromatic Hydrocarbon	Phenolic	Heterocyclic	Aliphatic
	Benzene, methyl–	Phenol	Acetophenone	2–methyl, 3–pentanone
	Benzene, ethyl–	Phenol, 2–methyl–	Furfural	n–docosane
	o–xylene	Phenol, 3–methyl–	(R)–benzyl–α–chloride	n–triacontane
	p–xylene	p–cresol, 2,2′–methylene bis(6–tert–butyl–)		Ethyl vinyl ketone
	m–xylene			
	Indane			
	Indene			
	Naphthalene			
	1,3,5–trimethylbenzene			
	p–ethyltoluene			

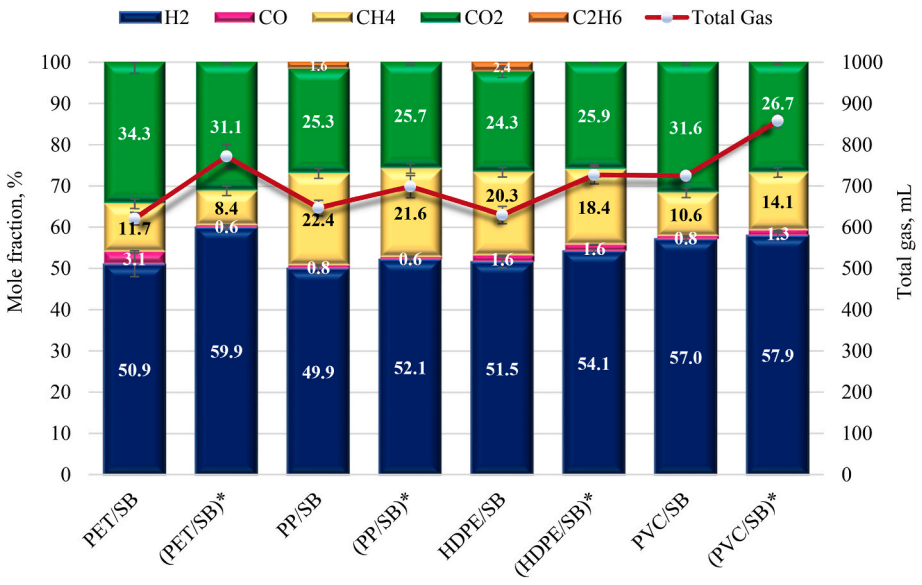


Fig. 3. The total gas volume and mole fractions of components from co–gasification of P/SB blends [P/SB* represents catalytic co–gasification results].

amount, it is thought that CO_2 supports methanation reaction [$CO_2 + 4H_2 \leftrightarrow CH_4 + 2H_2O$] and causes an increase in CH_4 amount [57]. Since a large portion of plastic waste reaches the oceans, KCl, which is abundant in seawater, was chosen as the catalyst. Evaluating it as an input without the need for additional processes such as desalination can contribute to the economic sustainability of high–cost hydrogen technologies. Fig. 4 shows the hydrogen efficiency for P/SB theoretical, non–catalytic, and catalytic co–gasification experiments for P/SB mixtures at 500 °C.

The data were analysed to identify the optimal conditions for hydrogen production efficiency. Hydrogen efficiency were expressed as the quantity of hydrogen generated per kilogram of feedstock (mol H_2/kg feed). For a better understanding of the effect of the catalyst in the experiments under the same conditions, individual experiments were also carried out with KCl. The theoretical data for the gasification of P/SB with KCl were given in Fig. 4 as H_2'*. The theoretical H_2 efficiencies of the co–gasifications were calculated using the H_2 efficiencies obtained from the individual experiments. When these results are evaluated, PVC/SB has the highest hydrogen efficiency after HcG of both uncatalysed and catalyzed blends. Co–gasification of PVC/SB without catalyst resulted in 16.9 mol H_2/kg feed. From the catalyzed HG of PVC alone, 12.8 (±0.2) mol H_2/kg feed and 10.8 (±0.4) mol H_2/kg feed were obtained from SB. The PVC/SB blend in the presence of KCl showed an increase of 8.4 mol H_2/kg feed compared to the theoretical value and 20.3 (±0.4) was obtained. From the catalyzed HG of PET alone, 10.5 (±0.3) mol H_2/kg feed and 10.8 (±0.4) mol H_2/kg feed were obtained from SB. The PET/SB blend showed an increase of 8.2 mol H_2/kg feed in the presence of KCl and 18.9 (±0.3) was obtained. HDPE/SB and PP/SB also showed an increase of 1–3 mol H_2/kg feed. The similar increase in total gas volume and hydrogen efficiency in both catalyzed and uncatalysed experiments can be attributed to the synergistic effect of both biomass and KCl in co–gasification. Table 3 presents the GC/MS analyses of the liquid products obtained after the non–catalytic co–gasification of P/SB. The percentage area was calculated relative to the total area.

The liquid products formed after P/SB non–catalytic co–gasification experiments consisted mostly of phenol (phenol, 24.4 min) and phenol derivatives (o–cresol, 32.4 min; 2,3 p–cresol, 33.9 min; 2,3–xylenol, 34.6 min; phenol, p–ethyl, 35.7 min; phenol, 4–ethyl–,1–acetate, 40.5 min; p–ethylguaiacol, 41.5 min). Although the components obtained as a result of liquid analysis were generally similar, the relative amounts of the products differed depending on the type of plastic used. Apart from phenol and its derivatives, other compounds detected in each combination; 5–hydroxy–2–heptanone (30.1 min) and furfural (14.7 min) in

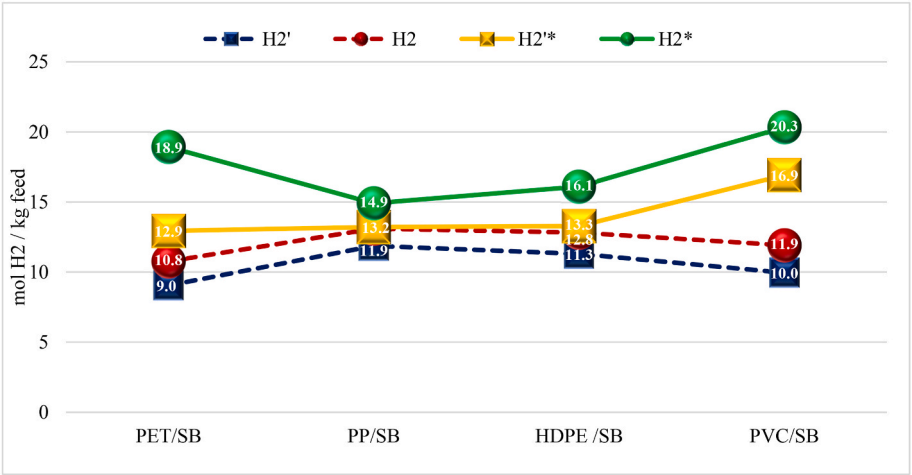


Fig. 4. The comparison of hydrogen efficiency for P/SB theoretical, non–catalytic, and catalytic co–gasification at 500 °C (H_2': theoretical non–catalytic, H_2: non–catalytic, H_2*': theoretical catalytic, H_2*: catalytic HcG results).

Table 3
GC–MS analysis of the liquid products obtained after non–catalytic co–gasification of P/SB at 500 °C.

RT	P/S (w/w)	Formula	PET/SB	HDPE/SB	PVC/SB	PP/SB
	Compound		Relative Abundance, %			
12.7	Toluene	C_7H_8	–	10.19	–	–
12.8	Ethyl vinyl ketone	C_5H_8O	–	3.19	3.82	2.93
14.7	Furfural	$C_5H_4O_2$	8.79	–	–	–
17.7	o–xylene	C_8H_{10}	–	7.28	–	2.77
22.6	2–furaldehyde,5–methyl–	$C_6H_6O_2$	2.04	–	–	–
24.4	Phenol	C_6H_6O	28.24	20.52	29.62	25.86
27.1	Benzyl alcohol	C_7H_8O	–	–	11.23	–
29.2	Acetophenone	C_8H_8O	7.46	–	–	–
30.1	5–Hydroxy–2–heptanone	C_7H_8O	20.90	2.02	–	1.48
32.4	o–cresol	C_7H_8O	–	12.43	20.12	13.56
33.9	p–cresol	C_7H_8O	–	15.79	4.24	23.02
34.6	2,3–Xylenol	$C_8H_{10}O$	2.39	–	–	–
35.7	Phenol, p–ethyl–	$C_8H_{10}O$	8.69	0.94	20.43	1.20
37.4	Benzoic acid	$C_7H_6O_2$	1.08	–	–	–
40.5	Phenol, 4–ethyl–,1–acetate	$C_{10}H_{12}O_2$	–	14.95	1.66	20.42
41.5	p–ethylguaiacol	$C_9H_{12}O_2$	1.28	–	1.38	–
	Other compounds		19.13	10.69	7.5	8.76

PET/SB mixture; toluene (12.37 min) and o–xylene (17.7 min) in HDPE/SB mixture; benzyl alcohol (27. 1 min) and p–ethylguaiacol (40.5 min); PVC/SB ethyl vinyl ketone (12.8 min) and 5–hydroxy–2–heptanone (12.8 min) were detected in PP/SB mixture. Table 4 shows the relative percentages of liquid products formed from the co–gasification of the P/SB mixture in the presence of a KCl catalyst.

When the co–gasification of PET/SB with and without catalyst is compared, it can be considered that the catalytic test environment triggers the conversion mechanism of the products into phenolic compounds (phenol and 2,3–xylenol) by promoting the decomposition of 5–hydroxy–2–heptanone. In the catalytic co–gasification of HDPE/SB blends, 1–hydroxymethyl furan was detected in the liquid phase. The main components obtained after catalytic gasification of PVC/SB, which is the combination with the highest decrease in liquid product diversity, belong to naphthalene derivatives (naphthalene, decahydro–, cis– and 1,2,3,4–tetrahydronaphthalene). Liquid analysis of this combination, which has the highest increase in total gas volume and H_2 % efficiency, is consistent. It was found that the liquid products obtained from catalytic co–gasification of PP/SB blends mainly consist of p–ethylphenol. It can be inferred that the KCl catalyst enhances hydrolysis and degradation reactions during the co–gasification of P/SB. This phenomenon can be attributed to the role of homogeneous alkali catalysts in promoting the cleavage of C–C bonds [51].

3.2. Temperature effect on catalytic co–gasification of SB with plastics

In this part of the study, PET, PP, HDPE, PVC catalyzed co–gasification with SB was carried out at 400, 450 and 500 °C. Thus, the contribution of temperature change in terms of improving possible experimental conditions can be interpreted. Fig. 5 shows the volumetric distribution of gasses obtained after HcG obtained from P/SB at different temperatures.

Under varying experimental conditions, hydrothermal water gasification can lead to different free radical and ionization reactions, which may occur in competition with one another. When the temperature approaches and exceeds the critical point, water becomes completely miscible with organic compounds due to its high solubility, low viscosity, decreasing dielectric constant and high diffusivity, and phase boundaries disappear [62,63]. Therefore, it is likely to penetrate structures such as decomposed long–chain hydrocarbons, polyene radicals, aromatics [64]. SB, which is rich in heteroatom content, is expected to decompose more easily with increasing temperature [52]. Compared to other P/SB combinations, Cl^- ions produced during hydrothermal dechlorination of PVC plastics may act as a catalyst promoting biomass decomposition [65], and this effect may increase with increasing temperature. In addition, there are heteroatoms in the main chain of PET and PVC polymers. However, the aromatic ring in the structure of PET is more stable. This structural difference may have affected the gasification efficiency of PET/SB. In the experiments with the same feedstock ratio and amount, the increase in H_2 efficiency as the temperature increases can be attributed to the increasing activity of water–gas reaction ($C + H_2O \leftrightarrow CO + H_2$) and steam–methane reforming ($CH_4 + H_2O \leftrightarrow CO_2 + 3H_2$) for a P/SB combination [59,66]. When temperature was increased from 400 °C to 450 °C, the H_2 volume for the PET/SB combination increased by 2.2 times. When the temperature was raised from 400 °C to 500 °C, 3.7–fold increase was observed, making the PET/SB combination the one with the highest H_2 volume increase among the tested plastics under these conditions. For the other P/SB combinations, these increase rates were obtained with 1.7–2.7–fold increases from 400 °C to 500 °C. The lower CO volume for each P/SB combination

Table 4
GC–MS analysis of the liquid products obtained from the KCl–catalyzed co–gasification of P/SB at 500 °C.

RT	Feedstock (w/w)	Formula	PET/SB	HDPE/SB	PVC/SB	PP/SB
	Compound		Relative Abundance, %			
24.4	Phenol	C_6H_6O	47.45	16.36	–	8.35
25.5	1–Hydroxymethyl furan	C_7H_8O	–	44.01	–	19.63
28.7	Benzenemethanol	$C_7H_{10}O$		16.13		
29.2	Acetophenone	C_8H_8O	–	–	–	12.03
30.3	Naphthalene,decahydro–, cis–	C_7H_8O	–	–	29.51	–
32.4	o–cresol	C_7H_8O	11.91	–	–	–
34.5	1,2,3,4–Tetrahydronaphthalene	$C_{10}H_{12}$	–	–	56.87	–
34.6	2,3–Xylenol	$C_8H_{10}O$	28.22	–	–	4.43
35.7	Phenol, p–ethyl–	$C_8H_{10}O$	–	10.57	–	36.43
41.5	p–ethylguaiacol	$C_9H_{12}O_2$	12.42	–	–	–
	Other compounds		–	12.93	13.62	19.13

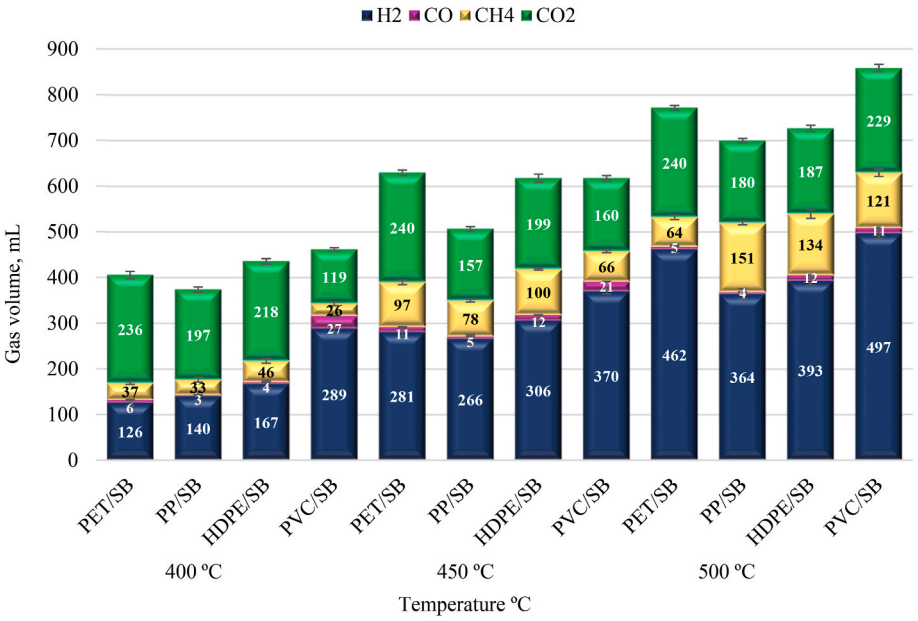


Fig. 5. The gas volume distributions from the HcG of PET, PP, HDPE, and PVC with SB at 400, 450, and 500 °C.

under increasing temperature conditions may be due to the consumption via water gas shift reaction ($CO + H_2O \leftrightarrow CO_2 + H_2$). In addition, the amount of CO tends to decrease or remain constant as the temperature increases due to its conversion to CO_2. The reason why the expected increase in the amount of CO_2 decreases or remains constant as the temperature increases is thought to be the increase in CO by promoting the Boudouard reaction ($C + CO_2 \leftrightarrow 2CO$) and again cyclically, it enters the water–gas shift reaction and increases the H_2 formation positively. As the temperature increases from 400 °C to 500 °C, the activity of the methanation reaction is observed to increase with increasing temperature for all co–gasification combinations. The gasification experiments conducted with KCl catalysts showed an increase in the total gas volume with a corresponding increase in hydrogen efficiency. Among the different temperatures studied, the PVC/SB blend exhibited the highest hydrogen production. The hydrogen efficiency ranking at 400 °C was observed as PVC/SB > HDPE/SB > PP/SB > PET/SB, while at 450 °C it followed the order PVC/SB > HDPE/SB > PET/SB > PP/SB. At 500 °C, the sequence was PVC/SB > PET/SB > HDPE/SB > PP/SB.

4. Conclusions

In this study, HG of PET, HDPE, PP, PVC with SB was carried out both separately and in combinations of P/SB. The effects of adding SB to the gasification of plastics on gasification performance, gas product distribution, H_2 efficiency, and liquid product distribution were investigated. Data obtained from trials without catalyst and with KCl catalyst were compared based on their contribution to H_2 efficiency. The effect of temperature on total gas volume and H_2 efficiency was investigated in catalyzed P/SB experiments conducted within the range of 400–500 °C. When comparing individual HG Results of plastics, PVC has the highest hydrogen mole fraction with 71.8 % (±1.7). However, the highest total gas volume (541 ± 24 mL) and H_2 volume (355 ± 9 mL) belonged to HG of PP. In P/SB combinations, the highest hydrogen efficiency was reached by increasing from 16.9 mol H_2/kg feed to 20.3 mol H_2/kg feed with the addition of KCl catalyst to HcG of PVC/SB. KCl supported the conversion of complex liquid by–products obtained from HcG trials into simpler compounds. While decreasing the presence of aromatic hydrocarbons and furfural in the liquid phase, it increased the formation of phenolic compounds. Furthermore, the PET/SB hydrogen efficiency in catalytic HcG increased by 6 mol/kg feed, which was the highest increase compared to other plastic combinations. The results obtained indicated that the use of KCl as a catalyst could be one of the suitable raw material input combinations for HG processes integrated with heat production or fuel synthesis from waste plastics. Considering the high cost of hydrogen production technologies in the use of waste plastic and energy biomass as inputs will significantly reduce the cost of the process. This study also provides critical insights into the role of biomass and alkali catalysts in improving the efficiency of hydrogen production from mixed plastic waste. The findings can guide the development of biomass integrated waste plastic management and energy recovery systems, contribute to environmental sustainability, and advance renewable energy technologies. Therefore, the study provides a basis for future research on H_2 production from similar plastic waste and energy products.

CRediT authorship contribution statement

Şefika Türker Üzden: Writing – review & editing, Writing – original draft, Visualization, Validation, Resources, Project administration, Investigation, Formal analysis, Conceptualization. **Ender Fakı:** Resources. **Açelya Seçer:** Writing – review & editing, Supervision. **Arif Hasanoğlu:** Writing – review & editing, Supervision, Project administration, Funding acquisition, Conceptualization.

Declaration of competing interest

The authors declare that they have no known competing financial interests or personal relationships that could have appeared to influence the work reported in this paper.

Acknowledgments

This study was funded by Çukurova University Research Grant, Turkey. (Project number: FDK–2020–13229).

Appendix A. Supplementary data

Supplementary data to this article can be found online at https://doi.org/10.1016/j.ijhydene.2025.02.179.

References

[1] Stubbins A, Law KL, Muñoz SE, Bianchi TS, Zhu L. Plastics in the earth system. Science 2021;373:51–5. https://doi.org/10.1126/SCIENCE.ABB0354/ASSET/B06675D9-0F84-4306-B875-8150320B2FF4/ASSETS/GRAPHIC/373_51_F4.JPEG. 1979.

[2] Global Plastics Outlook. Global plastics outlook. https://doi.org/10.1787/DE747AEF-EN; 2022.

[3] Stichnothe H, Azapagic A. Life cycle assessment of recycling PVC window frames. Resour Conserv Recycl 2013;71:40–7. https://doi.org/10.1016/J.RESCONREC.2012.12.005.

[4] Lewandowski K, Skórczewska K. A brief review of poly(vinyl chloride) (PVC) recycling. Polymers 2022;14:3035. https://doi.org/10.3390/POLYM14153035. 2022;14:3035.

[5] East AJ, Golder M, Makhija S. Polyesters, thermoplastic. Kirk-othmer encyclopedia of chemical technology. 2000. https://doi.org/10.1002/0471238961.1615122505011920.A01.

[6] Nisticò R. Polyethylene terephthalate (PET) in the packaging industry. Polym Test 2020;90:106707. https://doi.org/10.1016/J.POLYMERTESTING.2020.106707.

[7] Paul DR, Paul RD. Concise encyclopedia of polymer science and engineering, jacqueline I. Kroschwitz, john wiley & sons, New York, 1990. $135.00. JPoSB 1991;29:1653–4. https://doi.org/10.1002/POLB.1991.090291312.

[8] Geyer R, Jambeck JR, Law KL. Production, use, and fate of all plastics ever made. 2017.

[9] Global plastics production n.d. https://ourworldindata.org/grapher/global-plastics-production (accessed September 8, 2024).

[10] Zheng J, Suh S. Strategies to reduce the global carbon footprint of plastics. Nat Clim Change 2019;9(5):374–8. https://doi.org/10.1038/s41558-019-0459-z. 2019;9.

[11] Shams M, Alam I, Mahbub MS. Plastic pollution during COVID-19: plastic waste directives and its long-term impact on the environment. Environmental Advances 2021;5. https://doi.org/10.1016/j.envadv.2021.100119.

[12] Welden NA. The environmental impacts of plastic pollution. Plastic Waste and Recycling: environmental Impact. Societal Issues, Prevention, and Solutions 2020:195–222. https://doi.org/10.1016/B978-0-12-817880-5.00008-6.

[13] Hasanzadeh R, Mojaver P, Chitsaz A, Mojaver M, Jalili M, Rosen MA. Biomass and low-density polyethylene waste composites gasification: orthogonal array design of Taguchi technique for analysis and optimization. Int J Hydrogen Energy 2022;47:28819–32. https://doi.org/10.1016/j.ijhydene.2022.06.244.

[14] Mojaver M, Azdast T, Hasanzadeh R. Assessments of key features and Taguchi analysis on hydrogen rich syngas production via gasification of polyethylene, polypropylene, polycarbonate and polyethylene terephthalate wastes. Int J Hydrogen Energy 2021;46:29846–57. https://doi.org/10.1016/j.ijhydene.2021.06.161.

[15] Hasanzadeh R, Mojaver P, Khalilarya S, Azdast T. Air co-gasification process of LDPE/HDPE waste based on thermodynamic modeling: hybrid multi-criteria decision-making techniques with sensitivity analysis. Int J Hydrogen Energy 2023;48:2145–60. https://doi.org/10.1016/j.ijhydene.2022.10.101.

[16] Hasanzadeh R, Mojaver P, Azdast T, Khalilarya S, Chitsaz A. Developing gasification process of polyethylene waste by utilization of response surface methodology as a machine learning technique and multi-objective optimizer approach. Int J Hydrogen Energy 2023;48:5873–86. https://doi.org/10.1016/j.ijhydene.2022.11.067.

[17] A review on hydrothermal carbonization of biomass and plastic wastes to energy products [n.d].

[18] Modeling and process optimization of hydrothermal gasification for hydrogen production A comprehensive review [n.d].

[19] Onwudili JA, Williams PT. Catalytic supercritical water gasification of plastics with supported RuO2: a potential solution to hydrocarbons-water pollution problem. Process Saf Environ Prot 2016;102:140–9. https://doi.org/10.1016/j.psep.2016.02.009.

[20] Ha DT, Tong HD, Trinh TT. Insights into hydro thermal gasification process of microplastic polyethylene via reactive molecular dynamics simulations. Sci Rep 2024;14. https://doi.org/10.1038/s41598-024-69337-z.

[21] Ling M, Ma D, Hu X, Liu Z, Wang D, Feng Q. Hydrothermal treatment of polyvinyl chloride: reactors, dechlorination chemistry, application, and challenges. Chemosphere 2023;316. https://doi.org/10.1016/j.chemosphere.2022.137718.

[22] Boel MJ, Wang H, AL Farra A, Megido L, González-LaFuente JM, Shiju NR. Hydrothermal liquefaction of plastics: a survey of the effect of reaction conditions on the reaction efficiency. React Chem Eng 2024;9:1014–31. https://doi.org/10.1039/d2re00510g.

[23] Bai B, Wang W, Jin H. Experimental study on gasification performance of polypropylene (PP) plastics in supercritical water. Energy 2020;191. https://doi.org/10.1016/j.energy.2019.116527.

[24] Bai B, Liu Y, Wang Q, Zou J, Zhang H, Jin H, et al. Experimental investigation on gasification characteristics of plastic wastes in supercritical water. Renew Energy 2019;135:32–40. https://doi.org/10.1016/j.renene.2018.11.092.

[25] Cao C, Bian C, Wang G, Bai B, Xie Y, Jin H. Co-gasification of plastic wastes and soda lignin in supercritical water. Chem Eng J 2020;388. https://doi.org/10.1016/j.cej.2020.124277.

[26] Kruse A. Hydrothermal biomass gasification. J Supercrit Fluids 2009;47:391–9. https://doi.org/10.1016/j.supflu.2008.10.009.

[27] Türker Üzden Ş, Seçer A, Fakı E, Hasanoğlu A. Utilization of PET (waste) via hydrothermal co–gasification with sorghum for hydrogen rich gas production. J Energy Inst 2023;107. https://doi.org/10.1016/j.joei.2023.101193.

[28] Rasul MG, Hazrat MA, Sattar MA, Jahirul MI, Shearer MJ. The future of hydrogen: challenges on production, storage and applications. Energy Convers Manag 2022;272. https://doi.org/10.1016/j.enconman.2022.116326.

[29] Energy Agency I. Global hydrogen review 2024. 2024.

[30] Ismail MM, Dincer I. A new renewable energy based integrated gasification system for hydrogen production from plastic wastes. Energy 2023;270. https://doi.org/10.1016/j.energy.2023.126869.

[31] Yu H, Yang X, Jiang L, Chen D. Experimental study on Co-gasification characteristics of biomass and plastic wastes n.d.

[32] Pinto F, Franco C, André RN, Miranda M, Gulyurtlu I, Cabrita I. Co-gasification study of biomass mixed with plastic wastes. Fuel 2002;81:291–7. https://doi.org/10.1016/S0016-2361(01)00164-8.

[33] Burra KG, Gupta AK. Synergistic effects in steam gasification of combined biomass and plastic waste mixtures. Appl Energy 2018;211:230–6. https://doi.org/10.1016/J.APENERGY.2017.10.130.

[34] Lebreton LCM, Van Der Zwet J, Damsteeg JW, Slat B, Andrady A, Reisser J. River plastic emissions to the world's oceans. Nat Commun 2017;8. https://doi.org/10.1038/ncomms15611.

[35] Millero FJ, Huang F. Molal volumes and compressibilities of salts in seawater. Geochem Cosmochim Acta 2013;104:19–28. https://doi.org/10.1016/j.gca.2012.11.023.

[36] EA_POD_report_2024 [n.d].

[37] Geyer R, Jambeck JR, Law KL. Production, use, and fate of all plastics ever made. Sci Adv 2017;3. https://doi.org/10.1126/SCIADV.1700782.

[38] Duedall IW. Partial molal volumes of 16 salts in sea water. n.d.

[39] Millero FJ, Huang F. Molal volumes and compressibilities of salts in seawater. Geochem Cosmochim Acta 2013;104:19–28. https://doi.org/10.1016/j.gca.2012.11.023.

[40] House LR. Sorghum and millets: sorghum and millets: history, taxonomy, and distribution. n.d.

[41] Hasanzadeh R, Mojaver P, Azdast T, Chitsaz A, Park CB. Low-emission and energetically efficient co-gasification of coal by incorporating plastic waste: a modeling study. Chemosphere 2022;299:134408. https://doi.org/10.1016/J.CHEMOSPHERE.2022.134408.

[42] Phyllis2 - ECN Phyllis classification n.d. https://phyllis.nl/Browse/Standard/ECN-Phyllis#poly%20ethylene%20terephtalate (accessed September 8, 2024).

[43] Faki E, Üzden ŞT, Seçer A, Hasanoğlu A. Hydrogen production from low temperature supercritical water Co-Gasification of low rank lignites with biomass. Int J Hydrogen Energy 2022;47:7682–92. https://doi.org/10.1016/j.ijhydene.2021.12.125.

[44] Bandura AV, Lvov SN. The ionization constant of water over wide ranges of temperature and density. J Phys Chem Ref Data 2006;35:15–30. https://doi.org/10.1063/1.1928231.

[45] Čolnik M, Kotnik P, Knez Ž, Škerget M. Degradation of polyvinyl chloride (PVC) waste with supercritical water. Processes 2022;10:1940. https://doi.org/10.3390/PR10101940. 2022;10:1940.

[46] Boel MJ, Wang H, AL Farra A, Megido L, González-LaFuente JM, Shiju NR. Hydrothermal liquefaction of plastics: a survey of the effect of reaction conditions on the reaction efficiency. React Chem Eng 2024;9:1014–31. https://doi.org/10.1039/d2re00510g.

[47] Lopez G, Artetxe M, Amutio M, Alvarez J, Bilbao J, Olazar M. Recent advances in the gasification of waste plastics. A critical overview. Renew Sustain Energy Rev 2018;82:576–96. https://doi.org/10.1016/j.rser.2017.09.032.

[48] Ma D, Liang L, Hu E, Chen H, Wang D, He C, et al. Dechlorination of polyvinyl chloride by hydrothermal treatment with cupric ion. Process Saf Environ Prot 2021;146:108–17. https://doi.org/10.1016/j.psep.2020.08.040.

[49] Cao C, Bian C, Wang G, Bai B, Xie Y, Jin H. Co-gasification of plastic wastes and soda lignin in supercritical water. Chem Eng J 2020;388:124277. https://doi.org/10.1016/j.cej.2020.124277.

[50] Bodîrlău R, Teacă C-A, Spiridon I. Thermal investigation upon various composite materials, vol. 52; 2007.

[51] Rao YK, Adjorlolo A, Haberman JH. On the mechanism of catalysis of the Boudouard reaction by alkali-metal compounds. Carbon N Y 1982;20:207–12. https://doi.org/10.1016/0008-6223(82)90022-7.

[52] Hacisalihoglu G, Armstrong PR. Flax and sorghum: multi-element contents and nutritional values within 210 varieties and potential selection for future climates to sustain food security. Plants 2022;11:451. https://doi.org/10.3390/PLANTS11030451. 2022;11:451.

[53] Babatabar MA, Manouchehri M, Abbasi H, Tavasoli A. Supercritical water Co-gasification of biomass and plastic wastes for hydrogen-rich gas production using Ni-Cu/AC-CaO catalyst. J Energy Inst 2023;108:101251. https://doi.org/10.1016/J.JOEI.2023.101251.

[54] Di Blasi C, Branca C, Galgano A. Biomass screening for the production of furfural via thermal decomposition. Ind Eng Chem Res 2010;49:2658–71. https://doi.org/10.1021/IE901731U.

[55] Moghaddam L, Rencoret J, Maliger VR, Rackemann DW, Harrison MD, Gutiérrez A, et al. Structural characteristics of bagasse furfural residue and its lignin component. An NMR, py-GC/MS, and FTIR study. ACS Sustainable Chem Eng 2017;5:4846–55. https://doi.org/10.1021/ACSSUSCHEMENG.7B00274/SUPPL_FILE/SC7B00274_SI_001.PDF.

[56] Rostrup-Nielsen JR, Pedersen K, Sehested J. High temperature methanation. Sintering and structure sensitivity. Appl Catal Gen 2007;330:134–8. https://doi.org/10.1016/J.APCATA.2007.07.015.

[57] Le T, Striolo A, Turner CH, Cole DR. Confinement effects on carbon dioxide methanation: a novel mechanism for abiotic methane formation. Sci Rep 2017;7(1):1–12. https://doi.org/10.1038/s41598-017-09445-1. 2017;7.

[58] Mebrahtu C, Krebs F, Abate S, Perathoner S, Centi G, Palkovits R. CO 2 methanation: principles and challenges. Stud surf sci catal, vol. 178. Elsevier Inc.; 2019. p. 85–103. https://doi.org/10.1016/B978-0-444-64127-4.00005-7.
[59] Newsome DS. The water-gas shift reaction. Catal Rev 1980;21:275–318. https://doi.org/10.1080/03602458008067535.
[60] Byeon HJ, Jeon KW, Kim HM, Lee YH, Heo YS, Park MJ, et al. Promotion of methanation suppression by alkali and alkaline earth metals in Ni-CeO2 catalysts for water–gas shift reaction using waste-derived synthesis gas. Fuel Process Technol 2022;231. https://doi.org/10.1016/j.fuproc.2022.107229.
[61] Qiu Q, Pan D, Zhang W, Zeng F, Liu L. Catalytic kinetics and mechanisms of KCl with different concentrations on gasification of coal char. Processes 2022;10:1357. https://doi.org/10.3390/PR10071357. 2022;10:1357.
[62] Savage PE. Organic chemical reactions in supercritical water. Chem Rev 1999;99:603–21. https://doi.org/10.1021/cr9700989.
[63] Reddy S, Nanda S, Dalai A, of JK-IJ. Supercritical water gasification of biomass for hydrogen production. undefined. Elsevier; 2014. n.d..
[64] Wei N, Xu D, Hao B, Guo S, Guo Y, Wang S. Chemical reactions of organic compounds in supercritical water gasification and oxidation. Water Res 2021;190. https://doi.org/10.1016/j.watres.2020.116634.
[65] Braden J, Bai X. Production of biofuel precursor chemicals from the mixture of cellulose and polyvinylchloride in polar aprotic solvent. Waste Manag 2018;78:894–902. https://doi.org/10.1016/j.wasman.2018.07.011.
[66] Kim YG, Podolski WF. Modeling the water-gas shift reaction. Ind Eng Chem Process Des Dev 1974;13:415–21. https://doi.org/10.1021/I260052A021/ASSET/I260052A021.FP.PNG_V03.